Science Essence Journal Vol. 41 No. 1 (2025) | 51-64

Research Article

In Silico Investigation of Estrogen Receptor Alpha Inhibition by Alkyleneoxyberberine Derivatives

Natchaphon Ngueanngam[1], Benchawan Jityuti[1], Suwicha Patnin[2], Arthit Makarasen[2], Sucheewin Chotiwit[1], Siritron Samosorn[1] and Pornthip Boonsri[1*]

Received: 13 February 2025
Revised: 13 March 2025
Accepted: 14 March 2025

ABSTRACT

Breast cancer remains one of the most prevalent malignancies worldwide, with estrogen receptor alpha (ERα) playing a crucial role in its development and progression. In this study, we investigated the binding interactions and stability of berberrubine **(1)** and 9-(4-methyl phenethoxy) berberine **(2)** as potential ERα inhibitors using computational approaches. Molecular docking was performed to evaluate binding affinities and interactions, followed by molecular dynamics (MD) simulations to assess the stability and conformational changes of the ERα-ligand complexes. The binding free energy was further analyzed using Molecular Mechanics/Generalized Born Surface Area (MM-GBSA) calculations to identify key energy contributions. The results demonstrated that **(2)** exhibited stronger and more stable binding to ERα than **(1)**, though both were less potent than 4-hydroxytamoxifen **(OHT)**, a standard ERα inhibitor. Additionally, ERα-**(2)** interacts with key residues ALA350, GLU353, and ARG394, while exhibiting stronger van der Waals interactions than ERα-**(1)**, consistent with the MMGBSA energy component analysis. The study provides insights into the molecular mechanisms of ERα inhibition by berberine derivatives and highlights their potential as lead compounds for further development in breast cancer therapy.

Keywords: ER-alpha, Berberine, Molecular Dynamic, Molecular Docking, Molecular Mechanics/Generalized Born Surface Area (MM-GBSA)

[1]Department of Chemistry, Faculty of Science, Srinakharinwirot University, Bangkok 10110, Thailand
[2]Department of Chemistry, Laboratory of Organic Synthesis, Chulabhorn Research Institute, Bangkok 10210, Thailand
*Corresponding author, email: pornthipb@g.swu.ac.th

Introduction

Breast carcinoma is the most diagnosed cancer in women worldwide [1]. According to the statistical reports in 2018, the incidence of breast cancer in women was approximately 2.09 million cases around the world. [2]. However, early diagnosis and effective treatment can significantly reduce mortality rates. Discovering new compounds for the prevention and treatment of breast cancer is, therefore, critical in the medical field. To achieve this goal, the estrogen receptor (ER) is an important inhibition target, as it plays a role in the proliferation of breast tumor cells, which eventually leads to cancer metastasis [3].

ER-alpha (ERα) plays a crucial role in breast cancer research, as approximately 70% of diagnoses are related to this receptor, making it a key target for endocrine therapy to prevent the proliferation of breast cancers [3]. Anti-estrogen medicine, tamoxifen (TAM), is widely used in the treatment of breast cancers [4]. Although TAM demonstrates apparent anticancer effect, patients frequently develop resistance, which diminishes its therapeutic efficacy [5]. Thus, the development and synthesis of new compounds that specifically bind to ERα and inhibit estrogen-dependent proliferative activity are important and challenging for scientists.

Natural products have attracted considerable interest as new therapeutic agents because of their pharmacological properties, lower toxicity, and cost-effectiveness [6]. Several studies have indicated that natural compounds from fruits, vegetables, tea, coffee, spices, and medicinal plants can play a vital role in the prevention and treatment of cancers through various mechanisms of action [7]. Berberine, a natural alkaloid purified from the Berberis species, has demonstrated a wide range of pharmacological activities, including antibacterial, antihypertensive, anti-inflammatory, and antioxidative activities [6, 8, 9]. Furthermore, the anticancer effects and mechanisms of berberine have been extensively studied, with results suggesting that it could be a promising agent for the prevention and treatment of several cancers, such as breast, lung, gastric, liver, colorectal, ovarian, and prostate cancers [7, 10]. A report found that arylalkyleneoxyberberine derivatives could inhibit multiple types of cancer cells [11]. Furthermore, it showed greater potency than berberine and a number of anticancer drugs, suggesting that suitable modifications to the chemical structure of berberine may be crucial for the development of molecules with enhanced anticancer properties. Recently, Samosorn *et al.* investigated the anti-breast cancer activity of berberine derivatives on MCF-7 cells (unpublished data). The results indicated that 9-(4-methylphenethoxy) berberine (2) exhibited two fold higher potency than berberrubine (1). The structures of berberine derivatives (1) and (2) are shown in Figure 1.

Therapeutic compounds that selectively bind to ERα and inhibit estrogen-dependent proliferative activity are essential for developing promising treatment strategies because ERα plays important role in the initiation and progression of breast cancer [12]. In this study, we investigated the binding affinity and interactions of two berberine derivatives with ERα using computational approaches, including molecular docking, molecular dynamics (MD) simulations, and binding free energy calculations. These analyses offer valuable insights into the structure-activity relationship of

berberine derivatives, facilitating the rational design of more potent ERα inhibitors for breast cancer treatment.

Materials and Computational methods

2.1. Molecular docking studies

Molecular docking was employed to predict the intermolecular interactions and binding energies between each ligand as shown in the Figure 1 complexed to the estrogen receptor alpha (ERα) using Autodock 4.2 software [13]. The crystal structures of the ERα complexes were obtained from the Protein Data Bank (PDB) with the identification codes 3ERT (**ERα-OHT**). Preparation of the protein structure was carried out utilizing the BIOVIA Discovery Studio Visualizer 2024 software [14]. The structures of the newly synthesized berberine derivatives were optimized using density functional theory (DFT) with the B3LYP/6-31G(d,p) basis set, implemented in the Gaussian16 package. For the docking analysis, a three-dimensional grid box measuring 40 Å × 40 Å × 40 Å was set along the X, Y, and Z axes with a grid spacing of 0.375 Å. The grid box was centered at the binding sites of 3ERT. For the molecular docking calculations, a population size of 150 was used for the Genetic Algorithm (GA), with a maximum of 2,500,000 energy evaluations. The interactions of the docked conformations were visualized, and residue interactions were analyzed using the BIOVIA Discovery Studio 2024 program.

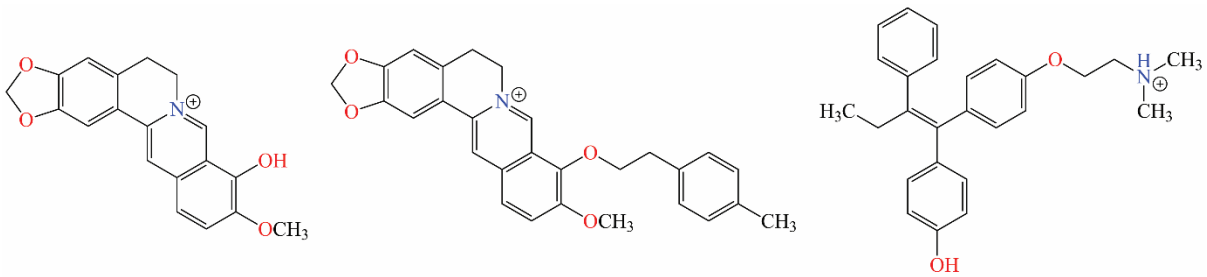

(1) **(2)** **(OHT)**

Figure 1 Molecular structures of berberine derivatives **(1)**, **(2)** and a standard ERα inhibitor as 4-hydroxytamoxifen **(OHT)**.

2.2. Molecular Dynamics Simulations

To understand the stability and interactions of the protein-ligand complexes, molecular dynamics (MD) simulations were applied to investigate ligand binding and protein folding within an optimized solvent environment. All MD simulations were conducted using the GROMACS 2023.5 software package [15]. The topologies for proteins and ligands were prepared using the AmberTools23 package, with the AMBER 19SB force field applied for the proteins [16]. The ligand force field parameters were generated using the General AMBER Force Field 2 (GAFF2), with charges calculated through Austin Model 1-bond charge corrections (AM1-BCC) via the Antechamber module. These complexes were positioned at the center of an octahedral box using the TIP3P water model [17], with

a spacing distance of 10 Å from the box edge. Additionally, the protonation state of ionizable residues was determined based on a pH of 7.4 using the PDB2PQR webserver [18]. The complex systems were neutralized by adding sodium and chloride ions to replicate a physiological salt concentration of 0.15 M. The AMBER topologies and coordinates of the complexes were generated and converted into GROMACS topologies using the ParmEd Python script. The energy minimization process employed the steepest descent algorithm, with a tolerance value of 10 kJ/mol/nm applied to the protein-ligand complexes. Subsequently, equilibration was performed using position restraints in the NVT ensemble, followed by the NPT ensemble, for a duration of 1000 ps. The production MD simulation was run for 100 ns, maintaining a temperature of 310 K and a pressure of 1 bar. Additionally, the MD simulation results were analyzed and visualization of the trajectory using the Visual Molecular Dynamics (VMD) program [19].

2.3. Binding free energy calculation

The binding free energy of the ERα-ligand complexes was calculated from the MD simulation trajectory using the widely adopted Molecular Mechanics/Generalized Born Surface Area (MM-GBSA) method, implemented using the gmx_MMPBSA package [19]. Binding free energy and per-residue decomposition analyses were performed on 3000 frames extracted from the stable phase of the simulation. The modified Generalized Born (GB) model 2 was utilized for the MMGBSA calculations [21]. Additionally, the solvation energy of the complexes was computed using the GB model with an implicit solvent dielectric constant of 78.5. The dielectric constant of the solute was set to 3, and the ionic strength was adjusted to 0.15 M to mimic physiological conditions. All calculations were performed with appropriate algorithms using a solvent probe radius of 1.4 Å and employed the Interaction Entropy (IE) method [22].

Results and Discussion

3.1 Molecular docking studies

Molecular docking, a widely utilized and efficient computational technique, was employed to investigate the binding energies and interactions between proteins and small molecules. To evaluate the inhibitory potential of arylalkylamine berberine derivatives against ERα, the best conformations obtained from molecular docking were selected for further assessment of stability and binding affinity through MD simulations. The docking results for the binding locations and affinities of **OHT** and both compounds bound to the ligand-binding domain (LBD) of ERα are shown in Figure 2. Additionally, the lowest binding free energies and interactions with amino acids within 3 Å are summarized in Table 1. The docking studies revealed that all ligands exhibited the lowest binding free energies when interacting with the LBD of ERα, as depicted in Figures 2B, 2C, and 2D. The binding energy values for the ERα-ligand complexes ranged from -8.56 to -11.32 kcal/mol, with ERα-**OHT** demonstrating the lowest binding energy at -11.32 kcal/mol, followed by ERα- **(2)** at -9.39 kcal/mol and ERα-**(1)** at -8.56 kcal/mol, respectively.

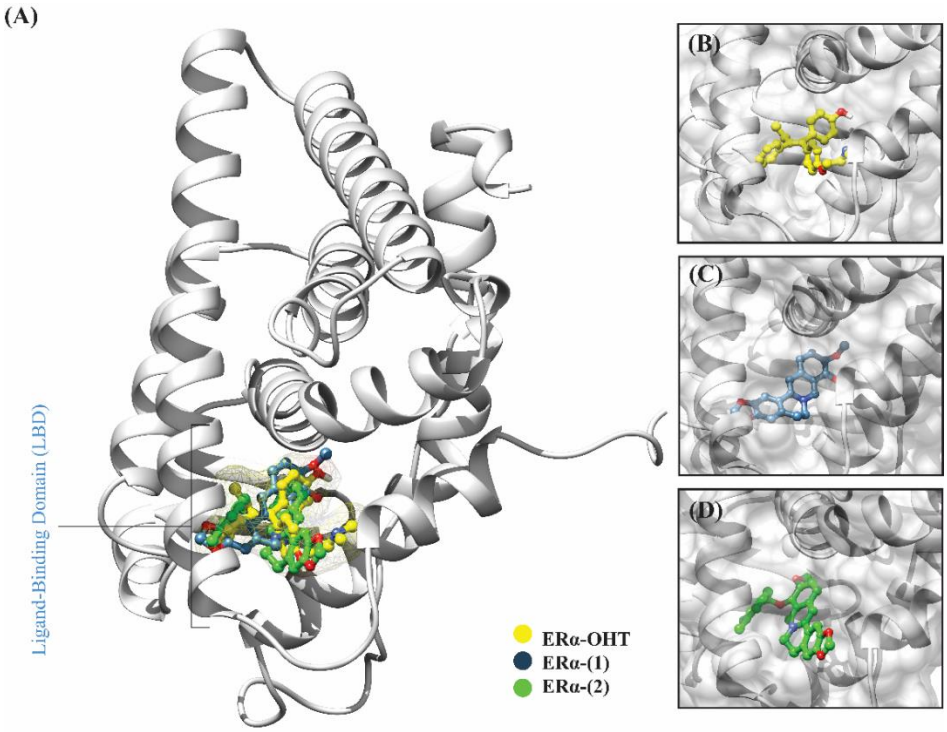

Figure 2 (A) Superimposition of **OHT** and berberine derivatives into the ERα within the ligand-binding domain (LBD). Binding pores of (B) ERα-**OHT**, (C) ERα-**(1)**, and (D) ERα-**(2)**, respectively.

Table 1 Binding interactions between interested ligands and ERα surrounding amino acids within 3 □.

Ligands	Binding energy (kcal/mol)	H-bonds	Hydrophobic Interactions
		Conventional H-bond	
(1)	-8.56	GLU353, ARG394	LEU387, LEU391, LEU525
(2)	-9.39	ALA350	LEU346, ALA350, LEU387, MET412, HIS524, ILE424, LEU525
OHT	-12.16	GLU353, ARG394	ALA350, LEU387, LUE346, MET421, PHE404

In the crystallographic structure of **OHT** bound to ERα, hydrogen bonding interactions with ALA350, GLU353, and ARG394 were observed [3, 23, 24]. Notably, a structural water molecule mediated a crucial H-bond interaction between these residues. Additionally, the H-bonding interaction between **OHT** and ASP351 played a significant role in inducing the displacement of helix 12 (H12), thereby disrupting coactivator binding [3, 23]. Hydrogen bonding interactions were identified between **OHT** and GLU353 and ARG394, whereas hydrophobic interactions involved PHE404, ALA350,

LEU387, and MET421, respectively. For compound **(1)**, hydrogen bonding was maintained with GLU353 and ARG394, while hydrophobic interactions were observed with residues such as LEU387, LEU391, and LEU525, respectively. Similarly, in the ERα**-(2)** complex, hydrogen bonding occurred with ALA350, whereas hydrophobic interactions involved MET412, LEU346, ALA350, LEU387, HIS524, ILE424, and LEU525, respectively. Moreover, comparing the binding energies of ERα**-(1)** and ERα**-(2)**, compound **(2)** exhibited a lower binding energy than compound **(1)**, suggesting that binding of ERα**-(2)** was more stable than that of ERα**-(1)**. To further investigate the stability of the ERα**-(2)** complex, molecular dynamics simulations and binding free energy calculations were performed to acquire a better understanding of the potential inhibitory effect on ERα.

3.2 Molecular dynamics (MD) simulations

Molecular dynamics (MD) simulations were performed to assess the stability of ligand binding to the protein, conformational changes, and protein folding within a solvated environment. The MD simulations provide a dynamic representation of all atoms in the protein, ligand, and solvent, enabling a more realistic and flexible analysis [25]. To evaluate the structural stability, several parameters were analyzed, including root mean square deviation (RMSD) of the protein backbone, root mean square fluctuation (RMSF), radius of gyration (Rg), and the number of hydrogen bonds.

The results of the MD simulations demonstrated the equilibrium and stability of ERα in complex with ligands, as shown in Figure 3. The RMSD analysis was used to evaluate the stability of ligand binding within the protein complex over the course of the simulation [26, 27]. Figure 3A illustrates the RMSD of the protein-ligand complexes, indicating that equilibrium was reached after approximately 20 ns. Interestingly, the ERα**-(2)** was the most stable complex throughout the simulation, with more stable fluctuations than ERα**-(1)** and minimal deviations in RMSD profile comparable to those observed with the ERα**-OHT** complex. This suggests that ERα**-(2)** maintains superior structural stability when the ligand is bound at the active site, making it a strong candidate for further investigation.

The RMSF plots indicate that lower fluctuations in the backbone residues correspond to stable interactions between the protein and ligand. In contrast, elevated fluctuations suggest increased structural flexibility, potentially indicating conformational changes within the protein [25, 26]. The flexibility of residues upon ligand binding was evaluated and is presented in Figure 3B. The analysis revealed a reduced flexibility of residues 350–371 and 388–410 in the ERα**-(2)** complex compared to ERα**-OHT**, suggesting enhanced structural stability due to the ligand binding of ERα. Similarly, the RMSF of the ERα**-(1)** complex exhibited greater fluctuations than both the ERα**-OHT** and ERα**-(2)** complexes. This indicated increased flexibility and suggested that the ERα**-(1)** complex was less stable than both the ERα**-OHT** and ERα**-(2)** complexes.

Additionally, the radius of gyration (Rg) is a key parameter for evaluating the compactness and stability of protein-ligand complexes, as it reflects fluctuations in the protein backbone within the

simulated systems. An increase in Rg fluctuations for the complex, compared to the unbound protein, suggests structural adjustments that contribute to stabilizing the interaction [28]. Figure 3C illustrates the radius of gyration (Rg) for ERα in the complexes with **OHT** and both berberine derivatives. The Rg plot of the ERα-**(2)** complex exhibited reduced fluctuations, nearly coinciding with that of ERα-**OHT**. This suggested that the increased compactness of **(2)** when bound to ERα contributed to the enhanced structural stability. Therefore, the MD simulation results indicated that the ERα-**(2)** complex was more stable than the ERα-**(1)** complex, consistent with the findings from the docking studies.

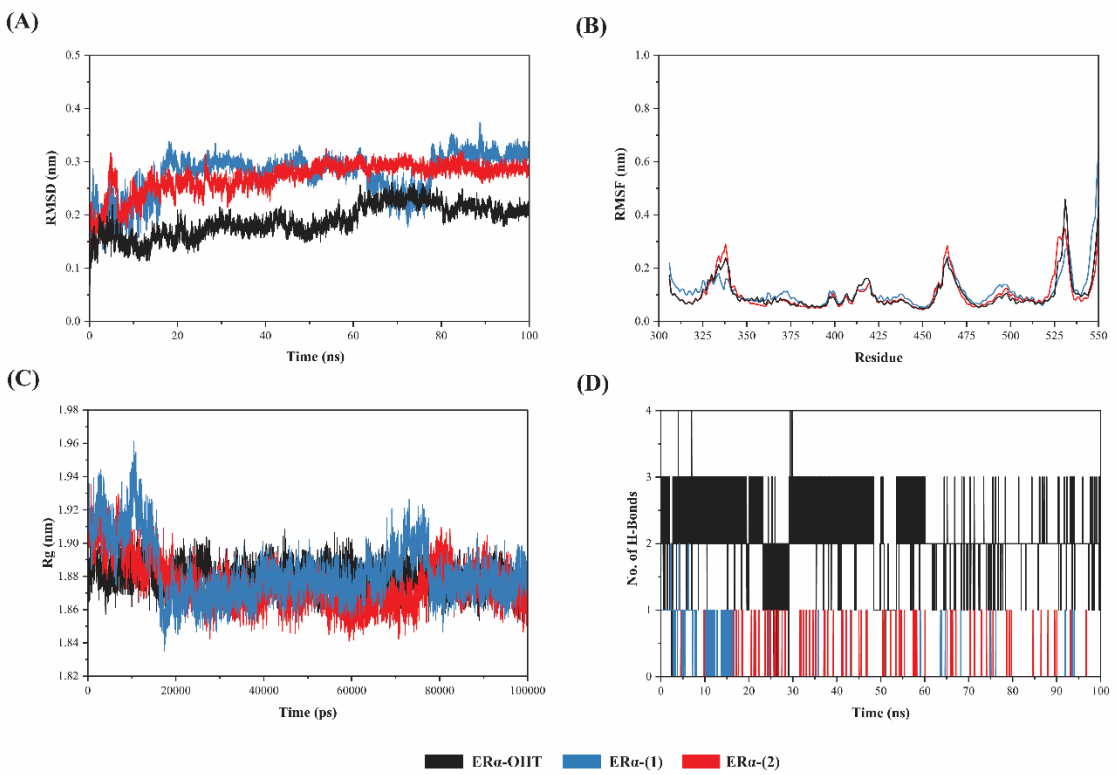

Figure 3 Analysis of the equilibrium and stability of ER-ligand complexes from MD simulations. (A) Backbone RMSD, (B) RMSF, (C) Radius of Gyration (Rg), and (D) the number of hydrogen bonds (No. of H-Bonds).

The number of hydrogen bonds (No. of H-Bonds) provides insight into the stability of ligand binding within the ERα complex over the course of the simulation, reflecting the dynamic nature of ligand-protein interactions. As shown in Figure 3D, ERα-**OHT** exhibited the highest consistency of hydrogen bonding interactions, indicating strong binding affinity. The ERα-**(2)** displayed frequent fluctuations in hydrogen bonding; however, the overall number of H-bonds remained relatively stable, suggesting a more stable binding mode compared to ERα-**(1)**.

3.3 Binding free energy calculation

The binding free energies between the ligands and ERα were determined using the Molecular Mechanics/Generalized Born Surface Area (MM-GBSA) method, considering various energy components, including van der Waals interactions, electrostatic interactions, solvation energies, and entropy contributions. To analyze the binding energies of the ERα-ligand complexes, 3000 frames from the final phase of the MD trajectory were extracted, and the MM-GBSA method was employed for calculations. This approach is widely used to compute binding free energies and per-residue free energy decomposition, providing deeper insights into molecular interactions and binding mechanisms. The individual energy components for both complexes are summarized in Table 2.

Table 2 Binding energies and individual component energy values obtained from the MM-GBSA calculation of, ERα with new synthesized compounds.

Energetic terms (kcal/mol)	(1)	(2)	OHT
ΔE_{vdw}	-36.59±3.56	-56.14±4.04	-54.49±3.66
ΔE_{ele}	-40.67±3.62	-42.72±2.87	-55.56±3.21
$\Delta G_{polar/GB}$	44.84±3.44	47.74±2.78	55.13±3.00
$\Delta G_{non\text{-}polar/GB}$	-4.42±0.66	-7.07±0.33	-7.64±0.27
-TΔS	9.11±0.05	10.44±0.05	10.34±0.05
$\Delta G_{bind/GB}$	-26.73±3.69	-46.76±4.18	-52.32±3.44

ΔE_{vdw} = van der Waals energy, ΔE_{elec} = electrostatic energy, $\Delta G_{polar/GB}$ = the polar solvation free energy obtained from the generalized Born method, $\Delta G_{non\text{-}polar/GB}$ = Nonpolar solvation free energy obtained from the generalized Born method, -TΔS = Interaction entropy, $\Delta G_{Binding/GB}$ = Total binding free energy (kcal/mol) from the generalized Born method.

According to the results, the binding free energies were evaluated using the Generalized Born (GB) models across the three complexes. In the MM-GBSA model, the binding free energies for ERα-**OHT**, ERα-**(1)**, and ERα-**(2)** were determined to be -52.32±3.44 kcal/mol, -26.73±3.69 kcal/mol, and -46.76±4.18 kcal/mol, respectively. The GB method approximated the effects of solvent molecules surrounding the complex using a simplified continuum model. These calculated binding energies indicate that the binding interaction of ERα-**(2)** is stronger than that of ERα-**(1)** but weaker than ERα-**OHT**. Notably, these findings were consistent with the binding energies obtained from molecular docking and the stability assessments derived from MD simulations. The van der Waals interaction energies for ERα-**OHT**, the ERα-**(1)** and ERα-**(2)** complexes were -54.49±3.66 kcal/mol, -36.59±3.56 and -56.14±4.04 kcal/mol, respectively. These interactions served as a key driving force in ligand binding, indicating strong hydrophobic interactions within the complexes. The ERα-**(2)** complex exhibited the most pronounced van der Waals interactions, even surpassing those of ERα-

OHT, suggesting that ERα-**(2)** formed stronger hydrophobic interactions within the ERα binding pocket. For electrostatic interaction energies, the **OHT**, **(1)**, and **(2)** complexes were found to be -55.56±3.21 kcal/mol, -40.67±3.62 kcal/mol, and -42.72±2.87 kcal/mol, respectively, highlighting the critical role of electrostatic forces in the binding process. In summary, both van der Waals and electrostatic interactions played essential roles in stabilizing the complexes, reinforcing their structural integrity through hydrophobic interactions and hydrogen bonding across all three systems.

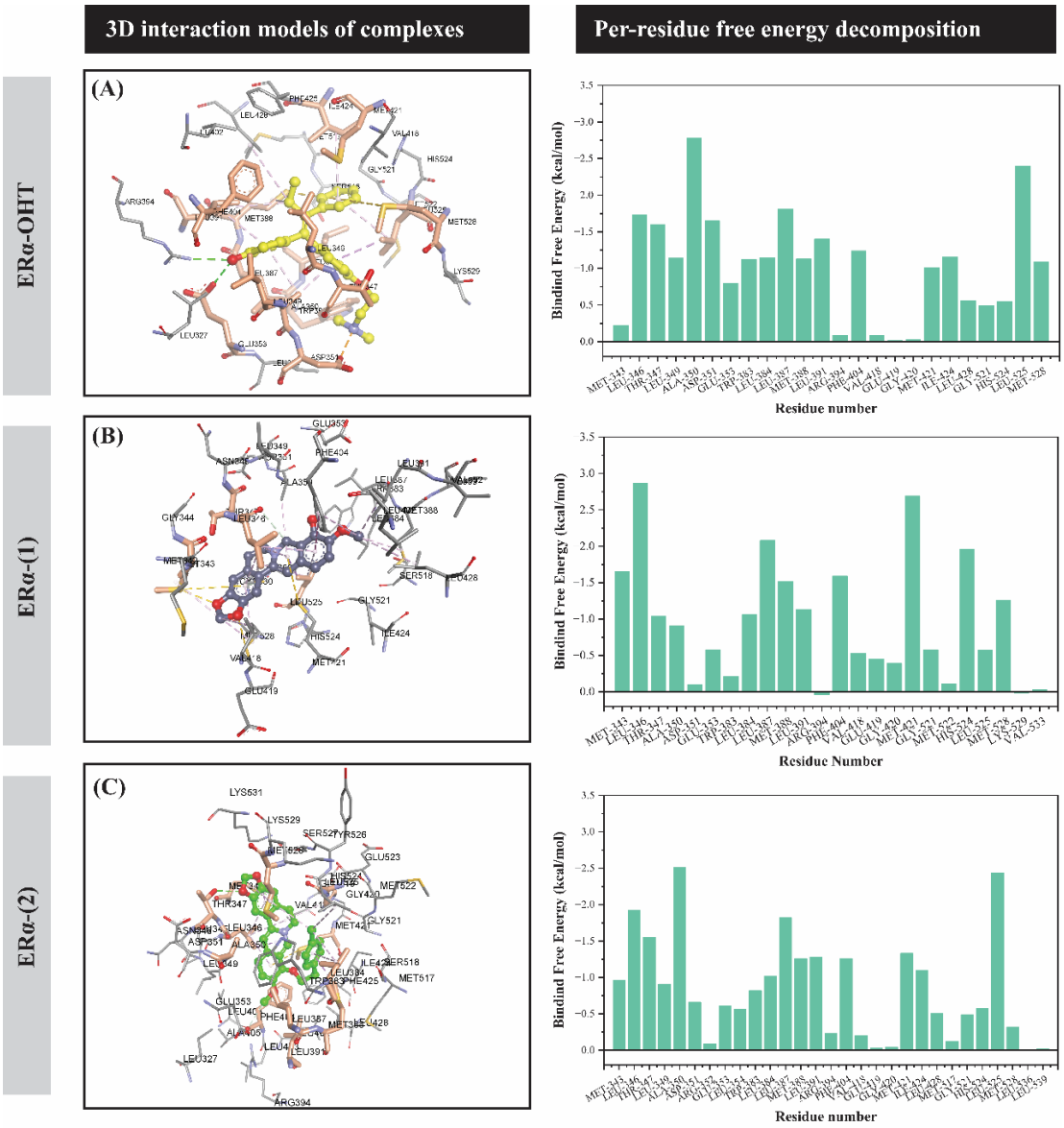

Figure 4 The energy decomposition and interaction analysis of the ERα structure for (A) the ERα-**OHT** complex, (B) the ERα-**(1)** complex, and (C) the ERα-**(2)** complex.

The energy decomposition contributions of ligand binding to ERα are presented in Figure 4. Residues with energy values of -1.0 kcal/mol or lower were analyzed to assess their role in stabilizing ligand interactions within the ligand-binding domain (LBD) of ERα [25]. This analysis identified key

residues that significantly contributed to ERα-**(2)** binding affinity, including MET343, LEU346, THR347, ALA350, LEU384, LEU387, MET388, LEU391, PHE404, MET421, which were similar to the ERα-**OHT**. Interestingly, ERα-**(2)** was able to establish interactions with all three key residues ALA350, GLU353, and ARG394. Additionally, ERα-**(2)** formed stronger van der Waals (vdW) interactions than ERα-**(1)**, as indicated by the number of interacting residues shown in Table 3. This result aligns well with the individual component energy analysis presented in Table 2. To understand the individual contributions of residues within the three complexes, representative cluster structures were generated from the MD trajectory. These findings provided valuable insights into the molecular interactions governing ligand binding and highlight the potential of these compounds as ERα inhibitors

Table 3 Individual residue interactions categorized by interaction type, extracted from the representative cluster of MD trajectories.

Compounds	van der Waals	H-Bond	Electrostatic		Hydrophobic			
		Carbon H-Bond	Sulfur-X	Pi-sulfur	Pi-Pi T	Pi-Sigma	Alkyl	Pi-Alkyl
(1)	HIS219, MET342, THR347, GLU353, LEU384, TRP383, LEU387, LEU402, GLU419, ILE424, GLY521,	LEU436	MET343, MET528,	MET343, MET421,	PHE404,	-	LEU346, MET343, LEU525, MET528, CYS530, VAL418, MET388, LEU391, LEU428,	ALA350, PHE404, LEU346 (2), LEU525 (2), MET528, CYS530
(2)	LEU327, LEU349, ALA350, GLU353, LEU387, LEU391, ARG394, LEU402, ALA405, ILE424, LEU428, MET388, LYS521, VAL418, SER527,	THR347, LYS531, PHE404	-	MET421,	-	LUE346,	LEU346, MET343, LEU525, MET528, LEU384	HIS219, MET343, LEU346, LEU348, MET528,

Conclusion

This study explored the potential of berberine derivatives as inhibitors of estrogen receptor alpha (ERα) through a computational approach. Molecular docking revealed that both **(1)** and **(2)** exhibited significant binding interactions within the ligand-binding domain (LBD) of ERα, though **(2)** demonstrated a stronger affinity than **(1)**. The molecular dynamics (MD) simulations further confirmed the stability of these interactions, with **(2)** maintaining structural integrity comparable to 4-hydroxytamoxifen **(OHT)**, a well-established ERα inhibitor. Binding free energy calculations using MM-GBSA provided additional insights into the driving forces behind ligand binding. Van der Waals and electrostatic interactions played a crucial role in stabilizing the complexes, with key contributions from residues such as ALA350, LEU387, and MET421. Especially, **(2)** exhibited stronger van der Waals interactions than **OHT**, indicating its potential for further development as an ERα inhibitor. This study provides a strong foundation for the rational design of ERα-targeting compounds, offering valuable insights into ERα inhibition and supporting the potential of berberine derivatives as candidates for breast cancer therapy.

Acknowledgements

The authors are grateful to the Chulabhorn Research Institute and Thailand Science Research and Innovation (TSRI) for financial support (Grant No. 49896/4759817 and 36824/4274395) during this study. Department of Chemistry, Faculty of Science, Srinakharinwirot University is gratefully acknowledged for providing research facilities.

References

1. Sun Y, Zhou Q, Chen F, Gao X, Yang L, Jin X, et al. Berberine inhibits breast carcinoma proliferation and metastasis under hypoxic microenvironment involving gut microbiota and endogenous metabolites. Pharmacol Res. 2023;193:106817.
2. Arbyn M, Weiderpass E, Bruni L, de Sanjosé S, Saraiya M, Ferlay J, et al. Estimates of incidence and mortality of cervical cancer in 2018: a worldwide analysis. Lancet Glob Health. 2020;8:e191-203.
3. Rocha-Roa C, Cortes E, Cuesta SA, Mora JR, Paz JL, Flores-Sumoza M, et al. Study of potential inhibition of the estrogen receptor α by cannabinoids using an in silico approach: agonist vs antagonist mechanism. Comput Biol Med. 2023;152:106403.
4. Patil JB, Kim J, Jayaprakasha GK. Berberine induces apoptosis in breast cancer cells (MCF-7) through mitochondrial-dependent pathway. Eur J Pharmacol. 2010; 645(1-3):70-8.
5. Pan X, Song Z, Cui Y, Qi M, Wu G, Wang M. Enhancement of sensitivity to tamoxifen by berberine in breast cancer cells by inhibiting ER-α36 expression. Iran J Pharm Res. 2022;21:e126919.

6. Jaitrong M, Boonsri P, Samosorn S. Molecular docking studies of berberine derivatives as novel multitarget PCSK9 and HMGCR inhibitors. Sci Ess J. 2021;37:124-42.
7. Xiong R-G, Huang S-Y, Wu S-X, Zhou D-D, Yang Z-J, Saimaiti A, et al. Anticancer effects and mechanisms of berberine from medicinal herbs: an update review. Molecules. 2022;27(14):4523.
8. Kuo H-P, Chuang T-C, Tsai S-C, Tseng H-H, Hsu S-C, Chen Y-C, Kuo C-L, Kuo Y-H, Liu J-Y, Kao M-C. Berberine, an isoquinoline alkaloid, inhibits the metastatic potential of breast cancer cells via Akt pathway modulation. J Agric Food Chem. 2012;60:9649-58.
9. Pan Y, Zhang F, Zhao Y, Shao D, Zheng X, Chen Y, He K, Li J, Chen L. Berberine enhances chemosensitivity and induces apoptosis through dose-orchestrated AMPK signaling in breast cancer. J Cancer. 2017;8:1679-89.
10. Xu J, Long Y, Ni L, Yuan X, Yu N, Wu R, et al. Anticancer effect of berberine based on experimental animal models of various cancers: a systematic review and meta-analysis. BMC Cancer. 2019;19(1):589.
11. Samosorn S, Tanwirat B, Suksamrarn A. Anticancer activity of 13-alkoxy berberine derivatives. Thai Patent 1101002293. 2011 Sep 27.
12. Sharma D, Kumar S, Narasimhan B. Estrogen alpha receptor antagonists for the treatment of breast cancer: a review. Chem Cent J. 2018;2(1):107.
13. Morris GM, Huey R, Lindstrom W, Sanner MF, Belew RK, Goodsell DS, et al. AutoDock4 and AutoDockTools4: Automated docking with selective receptor flexibility. J Comput Chem. 2009; 30(16):2785–91.
14. BIOVIA, Dassault Systèmes, Discovery studio visualizer, v20.1.0.19295. San Diego: Dassault Systèmes; 2020.
15. Abraham MJ, Murtola T, Schulz R, Páll S, Smith JC, Hess B, et al. GROMACS: high performance molecular simulations through multi-level parallelism from laptops to supercomputers. SoftwareX. 2015; 1:19–25.
16. Tian C, Kasavajhala K, Belfon KA, Raguette L, Huang H, Angela N, et al. ff9SB: amino-acid-specific protein backbone parameters trainedagainst quantum mechanics energy surfaces in solution. J Chem Theory Comput. 2019;16(1):528-52.
17. Mark P, Nilsson L. Structure and dynamics of the TIP3P, SPC, and SPC/E water models at 298 K. J Phys Chem A. 2001;105(43):9954–60.
18. Jurrus E, Engel D, Star K, Monson K, Brandi J, Felberg LE, et al. Improvements to the APBS biomolecular solvation software suite. Protein Sci. 2018;27(1):112-28.
19. Humphrey W, Dalke A, Schulten K. VMD: visual molecular dynamics. J Mol Grap. 1996;14(1):33–38.
20. Valdés-Tresanco MS, Valdés-Tresanco ME Valiente PA, Moreno E. gmx_MMPBSA: a new tool to perform end-state free energy calculations with GROMACS. J Chem Theory Comput. 2021;17(10):5969-6670.

21. Onufriev A, Bashford D, Case DA. Modification of the generalized Born model suitable for macromolecules. J Phys Chem B. 2000;104(15):3383-766.
22. Duan L, Liu X, Zhang JZH. Interaction entropy: a new paradigm for highly efficient and reliable computation of protein–ligand binding free energy. J Am Chem Soc. 2016;138(17):5465-728.
23. Shiau AK, Barstad D, Loria PD, Cheng L, Kushner PJ, Agard DA, et al. The structural basis of estrogen receptor/coactivator recognition and the antagonism of this interaction by tamoxifen. Cell. 1998;95(7):927–37.
24. Tanenbaum DM, Wang Y, Williams SP, Sigler PB. Crystallographic comparison of the estrogen and progesterone receptor's ligand binding domains. Proc Natl Acad Sci U S A. 1998;95(11):5998-6003.
25. Ding F, Peng W. Biophysical evaluation of protein structural flexibility for ligand biorecognition in solid solution. Phys Chem Chem Phys. 2016;18(9):6595-606.
26. Ngueanngam N, Jityuti B, Patnin S, Boonsri P, Makarasen A, Buranaprapuk A. Multiple spectroscopic and computational studies on binding interaction of 2-phenylamino-4-phenoxyquinoline derivatives with bovine serum albumin. Spectrochim Acta A Mol Biomol Spectrosc. 2024;310:123948.
27. Kooravand M, Asadpour S, Haddadi H, Farhadian S. An insight into the interaction between malachite green oxalate with human serum albumin: Molecular dynamic simulation and spectroscopic approaches. J Hazard Mater. 2021;407:124878.
28. Lobanov MY, Bogatyreva NS, Galzitskaya OV. Radius of gyration as an indicator of protein structure compactness. Mol Biol. 2008;42:623–8.